Environ. Sci. Technol. **2005**, *39,* 3069−3076

Simultaneous Utilization of Acetate and Hydrogen by *Geobacter sulfurreducens* and Implications for Use of Hydrogen as an Indicator of Redox Conditions

DERICK G. BROWN*

Department of Civil & Environmental Engineering, Lehigh University, 13 East Packer Avenue, Bethlehem, Pennsylvania 18015

JOHN KOMLOS AND PETER R. JAFFÉ

Department of Civil & Environmental Engineering, Princeton University, Princeton, New Jersey 08544

Dissolved hydrogen concentrations, in conjunction with other geochemical indicators, are becoming an accepted means to determine terminal electron acceptor processes (TEAPs) in groundwater aquifers. Aqueous hydrogen concentrations have been found to fall within specific ranges under methanogenic, sulfate-reducing, iron-reducing, and denitrification conditions. Although hydrogen is gaining in acceptance for determining subsurface TEAPs, there is a dearth of data with regards to the kinetic coefficients for hydrogen utilization in the presence or absence of an additional electron donor under different TEAPs. This study expands the kinetic data for hydrogen utilization through a series of batch experiments, which were conducted to study the utilization of acetate and hydrogen by *Geobacter sulfurreducens* under iron-reducing conditions. The results of these experiments indicate that the kinetic coefficients (cell yield and first-order degradation rate) describing the rate of hydrogen utilization by *G. sulfurreducens* under iron-reducing conditions correlate energetically with the coefficients found in previous experiments under methanogenic and sulfate-reducing conditions. In addition, with acetate and hydrogen as simultaneous electron donors, there is slight inhibition between the two electron donors for *G. sulfurreducens*, and this can be modeled through competitive inhibition terms in the classic Monod formulation. Finally, a key result of this study is that the TEAP-dependent hydrogen concentration in aquifers is not related solely to the microbial kinetics of the hydrogen-consuming organisms as previously suggested but is affected by the multi-substrate kinetics of hydrogen being consumed simultaneously with other electron donors as well as the availability of the electron acceptor.

Introduction

Hydrogen (H_2) and acetate have been shown to play important roles in the transformation of trace metals in subsurface environments, yet very little information is available regarding the kinetics of these processes as well as the effect, if any, of acetate on the kinetics of H_2 utilization and vice-versa when both electron donors are present and utilized simultaneously. One environmentally relevant example of the importance of H_2 utilization kinetics is that steady-state aqueous H_2 concentrations in groundwater have been shown to correlate with the dominant terminal electron accepting processes (TEAPs) in both pristine and contaminated aquifers (*1*−*3*).

TEAPs in groundwater aquifers typically vary based on the free-energy available from the reaction and order from aerobic > denitrifying > iron-reducing > sulfate-reducing > methanogenic conditions. TEAPs can vary over kilometers or more in pristine aquifers (*4*, *5*), to over a few meters in contaminated aquifers (*4*, *6*, *7*), to less than a meter vertically in aquatic sediments (*8*, *9*). In anaerobic environments, fermentation of organic matter, which can come from cell turnover or other sources, provides a ubiquitous source of hydrogen that can be used by different organisms as an energy source. Hydrogen concentrations have been measured in a wide diversity of aquifers and based on many field studies, aqueous hydrogen concentrations have been found to fall within specific ranges, with each range corresponding to a dominant TEAP (*2*, *6*). While these hydrogen concentrations appear to be due to the rates of microbial consumption of hydrogen as a function of TEAP, there is a dearth of data with regards to the kinetic coefficients for hydrogen utilization under different TEAPs. One key study examined hydrogen utilization under methanogenic and sulfate-reducing conditions (*10*). While this study provides evidence that the observed H_2 concentrations in the field are due to variation of kinetic coefficients with TEAP, due to a typographical error in Table 3 of that paper, the data has been inadvertently used to equate the hydrogen ranges observed in the field to those predicted with hydrogen used as the sole-substrate (e.g., through eq 2 below).

One practical application of H_2 measurements in the subsurface is to provide feedback for engineered control of TEAPs. Modification of TEAPs through injection of an electron donor, such as acetate, has show promise as a viable method for the immobilization of trace metals and radionuclides in the subsurface (*11*). Monitoring of the TEAP, such as through aqueous hydrogen concentrations, as electron donor is added is vital to the successful implementation of this technique. However, it is unknown how H_2 concentrations respond to the presence of additional electron donors during the biodegradation of trace metals, such as uranium and chromium, and how this may affect the observed correlation of H_2 concentration with TEAP.

The objectives of this research were to (a) determine kinetic parameters for microbial utilization of hydrogen under iron-reducing conditions and place these values in context of existing parameters for sulfate-reducing and methanogenic conditions; (b) determine kinetic parameters for simultaneous utilization of hydrogen and acetate under iron-reducing conditions; and (c) use these kinetic parameters with a multi-substrate biodegradation model to explore how the presence of an additional electron donor, such as acetate, may affect the utilization of hydrogen and hence the steady-state aqueous hydrogen concentrations. The research presented herein examined the effects of simultaneous hydrogen and acetate utilization through obtaining kinetic parameters under iron-reducing conditions in batch experiments. Soluble iron(III) citrate was used as the electron acceptor rather than solid iron(III) oxides to avoid surface-bound iron bioavail-

* Corresponding author phone: (610)758-3543; fax: (610)758-6405; e-mail: dgb3@lehigh.edu.

10.1021/es048613p CCC: $30.25
Published on Web 03/19/2005

ability limitations in order to focus on the effects of acetate on hydrogen kinetics during iron reduction. A model was formulated to describe the dual-electron donor utilization and the effects of an organic substrate on steady-state hydrogen concentrations were examined.

Theoretical Considerations

Single-Electron Donor H_2 Kinetics. The concept of dissolved hydrogen (H_2) serving as an indicator to predict the predominant TEAP in sediments resulted from the empirical observation that aquatic sediments with the same predominant TEAP had similar concentrations of dissolved hydrogen and that different TEAPs had distinct ranges of hydrogen concentrations associated with them. This observation was originally explained with a relatively simple model in which it was assumed that the uptake of hydrogen by a particular form of respiration follows Michaelis−Menten type kinetics, thus producing an equation for the steady-state hydrogen concentration that is independent of the rate of hydrogen production and solely dependent upon the physiological parameters of the hydrogen-consuming microorganisms (*3*). For example, Michaelis−Menten kinetics for steady-state bacterial concentration, where bacterial growth is balanced by endogenous decay, can be written as (*3*):

$$\frac{dX}{dt} = 0 = Y_{cell/H_2} V_{max}^{H_2} \frac{C_{H_2}}{K_m^{H_2} + C_{H_2}} X - bX \quad (1)$$

where X is the biomass concentration (no. of cells/mL); C_{H_2} is the aqueous hydrogen concentration (mol/L); $K_m^{H_2}$ is the hydrogen half-saturation constant (mol/L); $V_{max}^{H_2}$ is the maximum rate of hydrogen uptake (mol of H_2 (no. of cells)$^{-1}$ time^{-1}); Y_{cell/H_2} is the yield coefficient (no. of cells/mol of H_2); and b is the biomass endogenous decay coefficient (time^{-1}).

Solving for C_{H_2} gives the steady-state hydrogen concentration, which is often presented as the minimum substrate concentration required to maintain a stable microbial population:

$$C_{H_2} = \frac{bK_m^{H_2}}{Y_{cell/H_2} V_{max}^{H_2} - b} \quad (2)$$

This equation can also be written in terms of Monod kinetics by substituting $K_S^{H_2}$, the hydrogen half-saturation constant (mol/L), for $K_m^{H_2}$ and $\mu_{max}^{H_2}$, the maximum specific growth rate with hydrogen as the electron donor (time^{-1}), for $Y_{cell/H_2} \cdot V_{max}^{H_2}$. For the case of a pure culture with hydrogen as the sole electron donor, the hydrogen concentration that provides a steady-state biomass concentration can be determined via eq 2. While eq 2 does not predict the steady-state H_2 concentrations observed in the field (discussed below), it does predict the observed trends where sediments with more energetically favorable forms of respiration have lower steady-state hydrogen concentrations than sediments in which the respiration is less favorable.

H_2 Monod Kinetics for Two-Phase (Aqueous/Gaseous) System. In a system containing both gaseous (headspace) and aqueous hydrogen, hydrogen consumption can be written using Monod kinetics in terms of the total moles of hydrogen (H_T) in the system, with biodegradation only occurring in the aqueous phase:

$$\frac{dH_T}{dt} = -\frac{\mu_{max}^{H_2}}{Y_{cell/H_2}} \frac{C_{H_2}}{K_S^{H_2} + C_{H_2}} X V_{aq} \quad (3)$$

where the total moles of hydrogen in the reactor are defined as

$$H_T = C_{H_2} V_{aq} + C_{H_2}^{hs} V_{hs} \quad (4)$$

and where $C_{H_2}^{hs}$ is the H_2 concentration in headspace (mol/L); V_{aq} is the liquid volume (L); and V_{hs} is the headspace volume (L).

Equation 3 can be written in terms of the partial pressure of hydrogen in the headspace via the use of Otswalt's coefficient (*12*, *13*), which assumes equilibrium partitioning of hydrogen between the aqueous and headspace phases. Written in this manner, the model is a function of the experimentally obtained data (i.e., hydrogen partial pressure), and most importantly, it provides a simple means of accounting for the significant reservoir of H_2 in the headspace and its effect on the link between changes in the dissolved H_2 concentration and the biodegradation kinetics. Using Otswalt's coefficient and the ideal gas law, we can write

$$C_{H_2} = \left(\frac{L}{RT} P_{H_2}\right) \quad (5)$$

and

$$C_{H_2}^{hs} = \left(\frac{P_{H_2}}{RT}\right) \quad (6)$$

where L is Otswalt's coefficient for hydrogen (0.01887 at 30 °C) (*12*); P_{H_2} is the partial pressure of H_2 in headspace (atm); R is the universal gas constant (0.0821L·atm/K·mol); and T is the temperature (K).

Substituting eqs 4−6 into eq 3 results in the Monod equation written in terms of the partial pressure of hydrogen in the headspace:

$$\frac{dP_{H_2}}{dt} = -\frac{\mu_{max}^{H_2}}{\hat{Y}_{cell/H_2}} \frac{P_{H_2}}{\hat{K}_S^{H_2} + P_{H_2}} X \quad (7)$$

where the modified Monod parameters, written in terms of the partial pressure of hydrogen, are defined as

$$\hat{Y}_{cell/H_2} \equiv Y_{cell/H_2} \frac{V_{aq} L + V_{hs}}{V_{aq} RT} \quad (8)$$

$$\hat{K}_S^{H_2} \equiv K_S^{H_2} \frac{RT}{L} \quad (9)$$

The term $\hat{Y}_{cell/H_2}$ is the "observed" yield, which based solely on the measured hydrogen in the headspace (i.e., number of cells produced per atm of hydrogen removed from the headspace), while Y_{cell/H_2} is the "true" yield based on the total moles of hydrogen utilized in the reactor (i.e., number of cells produced per total mol of hydrogen consumed from entire reactor). In a similar manner, the Monod kinetics for biomass growth on hydrogen is given by

$$\frac{dX}{dt} = \mu_{max}^{H_2} \frac{P_{H_2}}{\hat{K}_S^{H_2} + P_{H_2}} X - bX \quad (10)$$

Dual-Electron Donor H_2 Kinetics. During a metal-radionuclide bioremediation scheme where an organic carbon source is injected into the subsurface, the simultaneous utilization of the carbon source and hydrogen is expected to affect the uptake kinetics of either substrate (*14*, *15*). At this time, little is known regarding the simultaneous utilization of carbon and hydrogen and their interactions on bacterial growth. Hydrogen has been shown to inhibit acetate degradation by *Methanosarcina thermophilia* (*16*) and to have minor inhibition on acetate degradation by *M. barkeri* and *M. mazei* (*17*). For this study, with acetate

used as the organic carbon source, it was hypothesized that the simultaneous acetate and hydrogen utilization can be described using competitive inhibition kinetics. This does not imply that acetate and hydrogen are competing in the sense of the classical Michaelis−Menten formulation. In a Monod formulation, which looks at a bacterium (or bacterial consortium) as a whole, the competitive inhibition model serves only as a general model of inhibition, as many enzymatic pathways are operational. Finally, a saturation kinetic term was included for the electron acceptor (in this case Fe^{3+}) in the Monod expression. Written in terms of the hydrogen partial pressure, in a manner similar to the derivation of eqs 7−10, gives the following system of equations:

$$\frac{dP_{H_2}}{dt} = -\frac{\mu_{max}^{H_2}}{Y_{cell/H_2}} \frac{P_{H_2}}{\hat{K}_S^{H_2} + P_{H_2} + \hat{K}_I^c C_c} \frac{C_{Fe^{3+}}}{K_{Fe^{3+}}^{H_2} + C_{Fe^{3+}}} X \quad (11)$$

$$\frac{dC_c}{dt} = -\frac{\mu_{max}^c}{Y_{cell/c}} \frac{C_c}{K_S^c + C_c + \hat{K}_I^{H_2} P_{H_2}} \frac{C_{Fe^{3+}}}{K_{Fe^{3+}}^c + C_{Fe^{3+}}} X \quad (12)$$

$$\frac{dC_{Fe^{3+}}}{dt} = \hat{Y}_{Fe^{3+}/H_2} \frac{dP_{H_2}}{dt} + Y_{Fe^{3+}/c} \frac{dC_c}{dt} \quad (13)$$

$$\frac{dX}{dt} = -\hat{Y}_{cell/H_2} \frac{dP_{H_2}}{dt} - Y_{cell/c} \frac{dC_c}{dt} - bX \quad (14)$$

where the modified Monod parameters, written in terms of the partial pressure of hydrogen, are defined as

$$\hat{Y}_{Fe^{3+}/H_2} \equiv Y_{Fe^{3+}/H_2} \frac{V_{aq}L + V_{hs}}{V_{aq}RT} \quad (15)$$

$$\hat{K}_I^c \equiv K_I^c \frac{RT}{L} \quad (16)$$

$$\hat{K}_I^{H_2} \equiv K_I^{H_2} \frac{L}{RT} \quad (17)$$

where C_c and $C_{Fe^{3+}}$ are the organic carbon and Fe^{3+} concentrations, respectively (mol/L); K_S^c is the half-saturation constant for acetate (mol/L); $K_{Fe^{3+}}^{H_2}$ and $K_{Fe^{3+}}^c$ are the half-saturation constants for iron reduction with hydrogen and acetate as the electron donors, respectively (mol/L); μ_{max}^c is the maximum specific growth rate on acetate ($time^{-1}$); $K_I^{H_2}$ (mol/L of acetate)/(mol/L of H_2) and K_I^c (mol/L of H_2)/(mol/L of acetate) are the competitive inhibition constants for hydrogen and acetate, respectively; $Y_{cell/c}$ is the bacterial cell yield coefficient (number of cells/mol of acetate); and Y_{Fe^{3+}/H_2} and $Y_{Fe^{3+}/c}$ are the yield coefficients, moles of iron(III) consumed per mole of hydrogen or acetate utilized, respectively (mole/mole). An advantage of the proposed multi-substrate utilization expressions is that the steady-state hydrogen concentrations representative for different TEAPs can be estimated from the knowledge of the degradation kinetics of the hydrogen source and the carbon source. This is accomplished similar to the derivation of eq 2 by setting eq 14 to zero and solving for the hydrogen concentration.

Materials and Methods

Bacterial Strain. *Geobacter sulfurreducens*, an obligate anaerobic bacterium, was used in this study. It was selected for its ability to reduce iron with either acetate or hydrogen, but not citrate, as electron donors (*18*). In addition, this organism was chosen because microorganisms with 16S rDNA sequences closely related to *G. sulfurreducens* are the predominant organisms in a variety of subsurface environments in which Fe^{3+} reduction is the predominant TEAP (*19*, *20*).

Media Composition and Preparation. All experiments used a defined ferric citrate media (*21*) containing 13.7 g of $FeC_6H_5O_7$, 2.5 g of $NaHCO_3$, 0.25 g of NH_4Cl, 0.6 g of $NaH_2PO_4 \cdot H_2O$, 0.1 g of KCl, 10 mL of vitamin solution (*21*), and 10 mL of trace minerals solution (*21*) per liter of distilled water. The ingredients (except the vitamin and mineral solutions) were combined and dissolved on a heated stir plate. The solution was then cooled, and pH was adjusted to ~7, followed by the addition of the vitamin and mineral solutions. Nine milliliters of solution was transferred to a 26 mL crimp-seal media tube, purged with CO_2/N_2 gas (20:80 ratio), sealed with a butyl rubber stopper, and autoclaved.

Batch Experiments. To maintain a constant inoculum of *G. sulfurreducens* for each experiment, growth cultures were prepared using the ferric citrate solution described above with hydrogen as the electron donor (initial hydrogen headspace concentration of 1 atm) and incubated at 30 °C. After 5 days of growth, 1 mL of growth culture was inoculated into media tubes containing the ferric citrate solution described above and supplied different concentrations of the electron donors hydrogen (~10^{-5} to ~10^{-2} atm, giving an initial aqueous concentration of ~0.01 to ~6.0 μM), acetate (0.74−8.6 mM) or a mixture of the two, depending on the specific experiment being conducted. These concentrations were selected to simulate conditions that might be seen during bioremediation schemes in the field (e.g., Anderson et al. used acetate concentrations of 1−3 mM; *11*). This resulted in 10 mL of solution and 16 mL of headspace (CO_2/N_2 gas at a 20:80 ratio) in the tubes. The test tubes were incubated at 30 °C, and separate test tubes were destructively analyzed for Fe^{2+}, acetate, hydrogen, and cell numbers at each time point. All test tubes inoculated with hydrogen were incubated on their side to maximize hydrogen diffusion from the headspace into solution. It was shown through screening experiments that shaking of the tubes did not affect the hydrogen biodegradation rate, indicating that diffusion of hydrogen from the headspace to the aqueous phase was not a rate-limiting step, and thus the equilibrium assumption used in development of the biodegradation model was valid for this system.

Analytical Techniques. Hydrogen was measured with gas chromatography using a reduced gas analyzer (Trace Analytical, Inc.). Iron reduction was quantified by measuring Fe^{2+} production over time using a modified version of the ferrozine method (*22*). Briefly, 0.1 mL of sample is added to 5 mL of 0.5 N HCl. After 15 min, 0.1 mL of the mixture is added to 5 mL of ferrozine solution (*22*), and the absorbance is measured at 562 nm (Spectronic Genesys 2 spectrophotometer was used in this study). Acetate concentrations were determined using ion chromatography (Dionex) with a Bio-Rad HPLC fast acid analysis column (100 × 7.8 mm).

For quantification of bacterial cell concentrations, 0.5 mL of bacterial suspension was fixed with 4.45 mL of 0.2 μm filtered oxalate solution (14 g of ammonium oxalate and 7.5 g of oxalic acid in 500 mL of H_2O) and 0.05 mL of 25% gutataric dialdehyde solution. The fixed cells were stained with 0.2 μm filtered 0.1% acridine orange solution (1.18 g acridine orange in 1000 mL H_2O), and counted using a Nikon epifluorescent microscope.

Parameter Estimation. Parameter estimation was carried out by developing a C-computer code based on eqs 11−14 and linking it to the model-independent nonlinear parameter estimation code PEST (Version 6.05, Watermark Numerical Computing). For this study, PEST was used to determine one set of Monod parameters that optimally fit multiple

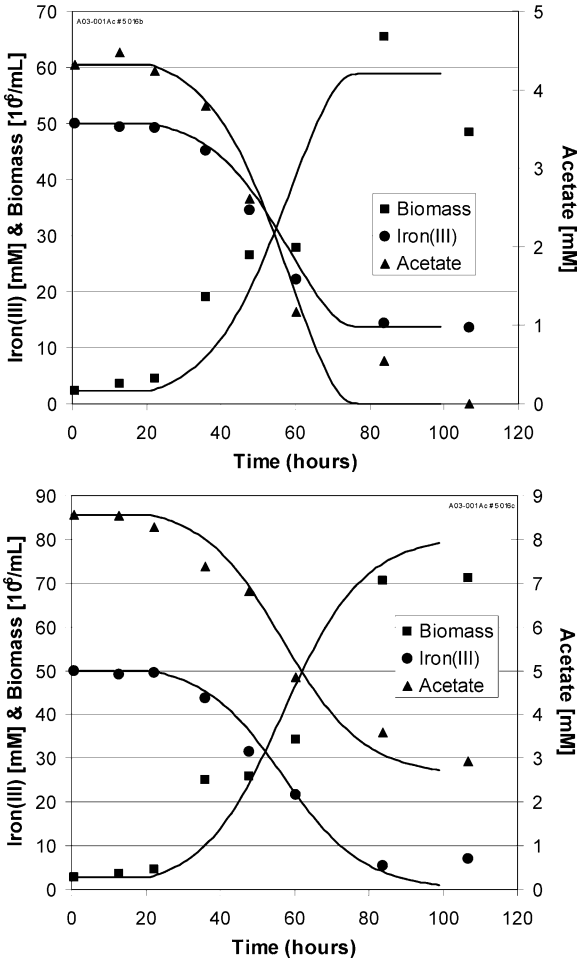

FIGURE 1. Two representative results for acetate consumption under Fe^{3+} reducing conditions. Symbols are experimental results. Lines are model results using parameters in Table 1.

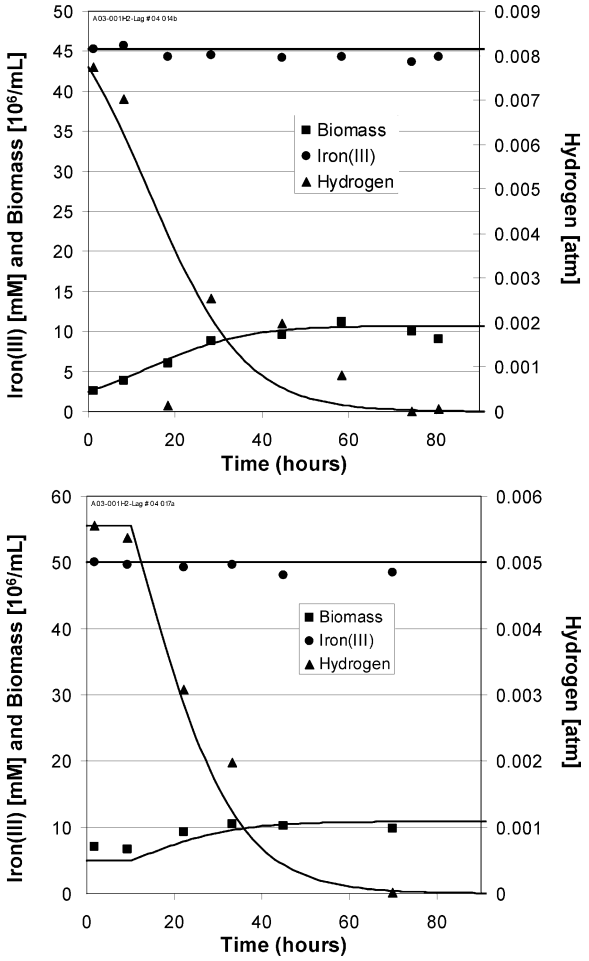

FIGURE 2. Two representative results for hydrogen consumption under Fe^{3+} reducing conditions. Symbols are experimental results. Lines are model results using parameters in Table 1.

experimental runs simultaneously. For example, results from multiple sole-electron donor experiments with acetate at varying initial concentrations were used simultaneously to develop one set of Monod parameters that optimally fit all the experimental results. Parameter estimations were carried out this way to determine Monod parameters for acetate and H_2 as sole electron donors. For this analysis, cell decay was neglected because of the short experimental durations (*23*). The sole-donor Monod parameters were then applied to the dual-donor experimental results, and PEST was used to determine one set of inhibition coefficients simultaneously for all dual-donor experiments.

Results

Single-Electron Donor Experiments. Three single-electron donor experiments were conducted with acetate as the electron donor at aqueous concentrations ranging from 0.74 to 8.6 mM. Five single-donor experiments were conducted with hydrogen as the electron donor at initial headspace partial pressures ranging from $\sim 10^{-5}$ to $\sim 10^{-2}$ atm (aqueous concentrations ranging from $\sim$0.01 to $\sim$6 μM). All experiments were carried out with Fe^{3+} as the electron acceptor, which was provided as ferric citrate. Representative results are shown in Figures 1 and 2 for acetate and hydrogen consumption, respectively, with additional results provided in the Supporting Information. These figures show the simultaneous depletion of electron donor (acetate or hydrogen) and Fe^{3+} and show the growth of biomass during suspended growth experiments with *G. sulfurreducens*. Control samples showed no abiotic loss of H_2 or acetate or production of Fe^{2+} during the course of the experiments (data not shown).

It was found during the biodegradation experiments that there was a constant lag period of approximately 21 h during all of the acetate biodegradation experiments, and this can be seen in Figure 1. A lag period was also observed for the hydrogen experiments. However, the lag period varied between experiments, ranging from no lag period to approximately 12 h, as seen in Figure 2. The observed lag periods for acetate and hydrogen were accounted for in the numerical model by delaying the start of the biodegradation until the end of the experimentally observed lag time (*24*−*26*), and the Monod parameters were determined as described above.

Monod parameters were estimated for the single-electron donor experiments using PEST. It was found during the parameter estimation process for hydrogen consumption that $\mu_{max}^{H_2}$ and $\hat{K}_S^{H_2}$ were very well correlated (correlation coefficient > 0.999), indicating that growth is first-order with respect to hydrogen for this experimental system. In addition, as shown in Figure 2, Fe^{3+} depletion was minimal during the hydrogen biodegradation experiments, and because of this, Monod parameters for Fe^{3+} could not be determined from the hydrogen data sets. Finally, during the acetate parameter estimation, it was found that μ_{max}^{c} and $K_{Fe^{3+}}^{c}$ were also very well correlated (correlation coefficient > 0.999), indicating that growth is first-order with respect to the iron concentration for this experimental system. With these correlations, eqs 11 and 12 can be rewritten as follows, where the terms in brackets are considered as one parameter:

TABLE 1. Kinetic Parameters of *G. sulfurreducens* during Iron Reduction with Acetate and/or Hydrogen as the Electron Donor[a]

acetate		hydrogen	
parameter	**value**	**parameter**	**value**
$\mu^{c}_{max}/K^{c}_{Fe^{3+}}$	0.00184 (h mM)$^{-1}$	$\mu^{H_2}_{max}/K^{H_2}_{S}$	12.2 (h mM)$^{-1}$
$Y_{cell/c}$	11.03 10^9 cells/mmol of acetate	Y_{cell/H_2}	16.3 10^9 cells/ mmol of H_2
K^{c}_{S}	0.124 mM	$K^{H_2}_{Fe^{3+}}$	nd
$Y_{Fe^{3+}/c}$	8.39 mM Fe^{3+}/mM acetate	Y_{Fe^{3+}/H_2}	nd
$K^{c}_{I}/K^{H_2}_{S}$	0.271 (mM acetate)$^{-1}$	$K^{H_2}_{I}$	959 mM acetate/mM H_2

[a] Parameters are specified for aqueous hydrogen concentrations. Parameters in terms of headspace hydrogen can be calculated with eqs 8, 9, and 15−17. All parameters except $K^{c}_{I}/K^{H_2}_{S}$ and $K^{H_2}_{I}$ were obtained from single-donor experiments. nd = not determinable.

$$\frac{dP_{H_2}}{dt} = -\frac{1}{Y_{cell/H_2}}\left[\frac{\mu^{H_2}_{max}}{\hat{K}^{H_2}_{S}}\right]\frac{P_{H_2}}{1+\left[\frac{\hat{K}^{c}_{I}}{\hat{K}^{H_2}_{S}}\right]C_c}X \quad (18)$$

$$\frac{dC_c}{dt} = -\frac{1}{Y_{cell/c}}\left[\frac{\mu^{c}_{max}}{K^{c}_{Fe^{3+}}}\right]\frac{C_c C_{Fe^{3+}}}{K^{c}_{S} + C_c + \hat{K}^{H_2}_{I}P_{H_2}}X \quad (19)$$

Monod parameters estimated from the experimental results are given in Table 1. Model results using these Monod parameters are included in Figures 1 and 2.

Dual-Electron Donor Experiments. Three dual-donor experiments were conducted with both acetate and hydrogen available as electron donors. Representative results are shown in Figure 3, with additional results provided in the Supporting Information. Using the single-donor Monod parameters in Table 1, the inhibition parameters ($K^{H_2}_{I}$ and $K^{c}_{I}/K^{H_2}_{S}$) were estimated simultaneously by PEST from these three data sets. These parameters are shown in Table 1. Figure 3 shows the experimental data along with the model results with and without inhibition (i.e., $K^{H_2}_{I} = K^{c}_{I} = 0$). Analysis of the weighted-least-squares residuals between the experimental data and the model results showed that there is a minor decrease in residuals when including the inhibition terms. Residuals for acetate, hydrogen, and iron were reduced, with the largest contribution being from iron, while those for biomass increased. This suggests that slight inhibition may be occurring between hydrogen and acetate under the conditions of these experiments.

Discussion

Knowledge of the kinetic parameters for hydrogen degradation under various TEAPs is required to estimate the steady-state hydrogen concentration as a function of the TEAP. Kinetic parameters have been previously determined for hydrogen utilization under methanogenic and sulfate-reducing conditions, and these results are presented in Table 2 along with the results of this study for hydrogen utilization under iron-reducing conditions. One would expect the first-order growth rate to vary as a function of the potential energy yield, and this is seen in Table 2, where the cell yield coefficient and first-order growth rate increase with potential energy yield for hydrogen utilization under methanogenic, sulfate-reducing, and iron-reducing conditions. Additionally, the cell yield varies linearly with the first-order growth rate for hydrogen utilization with these three electron acceptors (R^2 = 0.990).

The experimental cell yield from this study can also be compared to the theoretical yield estimated from the biological stoichiometry for hydrogen utilization under iron-reducing conditions. This can be calculated following the procedure outlined by Rittmann and McCarty (*27*), where the electron transfer between catabolic and anabolic reactions is used to determine an overall stoichiometric equation. Assuming a cell formula of $C_5H_7O_2N$, aqueous Fe(III), and a cell electron-transfer efficiency of 60% (*27*, *28*), the following stoichiometric equation can be obtained:

$$0.5H_2 + 0.764Fe^{3+} + 0.0118NH_4^{+} + 0.0118HCO_3^{-} + 0.0472CO_2 \rightarrow 0.0118C_5H_7O_2N + 0.106H_2O + 0.764H^{+} + 0.764Fe^{2+} \quad (20)$$

With the cell molecular weight of 113 g/mol, and assuming 0.55 g of protein/g of cells (*29*), the theoretical bacterial cell yield for growth on H_2 is 1.5 g of protein/mol of H_2. This value is within a factor of 2 of the experimental yield of 2.5 g of protein/mol of H_2 (Table 2), which is very reasonable given the assumptions made in the theoretical calculations.

For the acetate kinetic parameters, the Fe^{3+} utilization as a function of acetate was found to be 8.39 mM Fe^{3+}/mM acetate and is similar to the value of 6.8 mM Fe^{3+}/mM acetate found for *G. sulfurreducens* by Caccavo et al. (*18*). The cellular yield as a function of Fe^{3+} utilization was found to be 1.31 × 10^9 cells/mmol of Fe^{3+}, where

$$Y_{cell/Fe^{3+}} = \frac{Y_{cell/c}}{Y_{Fe^{3+}/c}} \quad (21)$$

This value is similar to cellular yield values reported for *S. putrefaciens* using ferric citrate with lactate as the electron donor (1.28 × 10^9 cells/mmol of Fe^{3+} (*30*) and 5.24 × 10^9 cells/mmol of Fe^{3+} (*26*)).

Geobacter sulfurreducens utilized acetate and H_2 simultaneously with ferric citrate as the electron donor. The presence of acetate resulted in only slight inhibition of the kinetics of H_2 utilization and vice-versa during iron reduction. This is a favorable finding, because if there were strong inhibition, then the use of H_2 as an indicator of TEAP may fail during biostimulation schemes. It should be noted that inhibition of acetate biodegradation by H_2 has been reported at higher H_2 concentrations. Ahring et al. (*16*) reported that H_2 concentrations above ∼2 μM showed signs of inhibition on acetate degradation by *Methanosarcina thermophila*, and above ∼15 μM H_2 completely inhibited acetate degradation. Boone et al. (*17*) reported little effect of H_2 on the rate of cell growth on acetate for *M. barkeri* and *M. mazei* at H_2 concentrations up to ∼6 μM. To our knowledge, the current study is the first to compare the impact of acetate and hydrogen on the kinetics of each other during iron reduction.

As mentioned above, the steady-state dissolved hydrogen concentrations for different TEAPs are dependent on the physiological parameters of the hydrogen-consuming organisms. Application of eq 2, where H_2 is the sole electron donor, does predict the trends seen in the field (Table 3), where hydrogen concentrations decrease with increasing potential energy of reaction. However, as shown in Table 3, the steady-state hydrogen concentrations predicted with eq 2 are 2−3 orders of magnitude greater than those values observed in the field. An obvious explanation for this discrepancy is that the kinetic coefficients measured in the

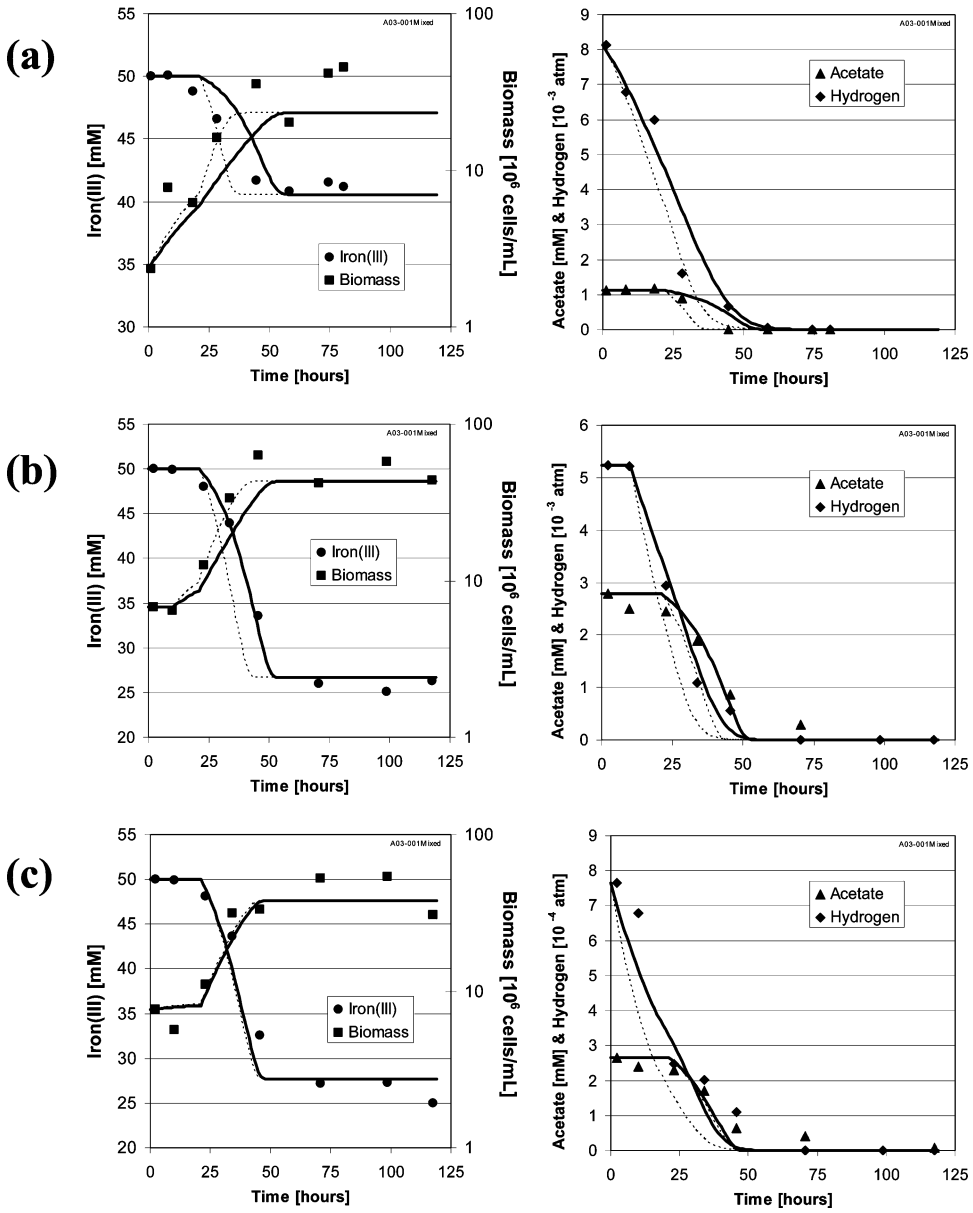

FIGURE 3. Dual-electron donor experiments with simultaneous utilization of acetate and hydrogen. Solid symbols are experimental results. Lines are model results using parameters in Table 1 with inhibition (solid) and without inhibition (dashed). Initial conditions are (a) 1 mM acetate and 0.008 atm H_2; (b) 3 mM acetate and 0.005 atm H_2; and (c) 3 mM acetate and 0.0008 atm H_2.

laboratory under ideal growth conditions differ from those in the field. In addition, it is possible that in the field there are mechanisms driving the steady-state hydrogen concentrations down from those predicted by eq 2, where hydrogen is the sole growth substrate. One possible mechanism is the interaction of H_2 with additional electron donors. Hydrogen is usually not the sole electron donor present where field observations of H_2 concentrations have been correlated to TEAPs. Other electron donors include petroleum hydrocarbons in contaminated aquifers (*4*, *31*−*33*) or natural organic matter in pristine aquifers (*4*). In addition, fermentation of organic matter is not only a source of H_2, but also of additional fermentation products, such as acetate, which can serve as electron donors for TEAPs. Limiting concentration of electron acceptor is another possible mechanism that can influence the steady-state H_2 concentration.

To achieve a steady-state hydrogen concentration when a second electron donor is present, overall bacterial growth on both donors must be balanced by the endogenous decay (i.e., $dX/dt = 0$ in eq 14). This is demonstrated in Figure 4, where eq 14 was used to determine steady-state hydrogen concentrations under iron-reducing conditions at various acetate and Fe^{3+} concentrations using the kinetic coefficients in Table 1 and endogenous decay in Table 2. Figure 4a presents the steady-state hydrogen concentrations when there is no inhibition between acetate and hydrogen. When the Fe^{3+} concentration is low, the steady-state hydrogen concentrations become asymptotic as the acetate concentration increases. In this case, iron is limiting, and any increase in acetate concentration $\gg K_S^c$ has no effect on the overall growth rate. However, as iron becomes less limiting, there is a maximum acetate concentration that will allow steady-state conditions to exist, as indicated by the sharp drop-off of hydrogen concentrations with increasing acetate concentration. If the acetate concentration is higher than this asymptotic value, then steady-state conditions do not exist, and the biomass is growing faster than its decay rate (i.e., $dX/dt > 0$). For the case where the acetate concentration is $\ll K_S^c$, the steady-state hydrogen concentration approaches the value predicted by eq 2, where hydrogen is the sole

TABLE 2. Potential Energy of Reaction, Cell Yield Coefficient, and First-Order Growth Rates for Different Terminal Electron Acceptor Processes with Hydrogen as the Sole Electron Donor

TEAP	$\Delta G^{\circ\prime}$ (kJ/mol of H_2)	Y_{cell/H_2} (g of protein/ mol of H_2)	$[\mu_{max}^{H_2}/K_S^{H_2}]^c$ or $[V_{max}^{H_2}Y/K_m^{H_2}]^b$ $(h\ \mu M)^{-1}$	b $(h)^{-1}$
methanogenesis	−34[a]	0.20[b]	3.22×10^{-4} [b]	0.00042[a]
sulfate reduction	−38[a]	0.85[b]	4.68×10^{-3} [b]	0.00042[a]
iron reduction	−228[a]	2.5[c,d]	1.20×10^{-2} [c]	0.00042[a]

[a] Ref *13*. $\Delta G^{\circ\prime}$ for iron reduction is for soluble Fe(III). $\Delta G^{\circ\prime}$ for iron hydroxides is an order of magnitude lower (e.g., −50 kJ/mol H_2 for $Fe(OH)_3$ (*3*)). [b] Ref *10*. Used Michaelis−Menten coefficients from this manuscript, as the authors considered their Monod coefficients to be general estimates. $V_{max}^{H_2} = 0.11\ \mu mol\ min^{-1}\ mg^{-1}$ for both methanogens and sulfate-reducers and $K_m = 4.1\ \mu M$ for methanogens and 1.2 μM for sulfate-reducers. Note that the yield coefficients given in Table 3 of this reference are a typographical error. The correct values are presented above. [c] This research. [d] 1 cell = 2.8×10^{-13}g and 1 g of cell = 0.55 g of protein (for *E. coli* cell) (*29*).

TABLE 3. Steady-State Hydrogen Concentrations with (i) Field Data Taken from the Literature and (ii) Hydrogen as the Sole Electron Donor[a]

	methanogenesis (nM)	sulfate reduction (nM)	iron reduction (nM)
field data[b]	5−30	1−4	0.2−0.8
H_2 as sole electron donor[c]	1,305	90	52

[a] Values calculated using parameters in Table 2. [b] Ref *36*. [c] Calculated from eq 2.

electron donor. Figure 4b presents the same conditions as Figure 4a but includes inhibition between acetate and hydrogen (Table 1). A similar drop-off in steady-state hydrogen concentrations is seen for the higher iron concentrations as Figure 4a. However, in contrast to Figure 4a, steady-state hydrogen concentrations rise above the value predicted via eq 2 as iron becomes more limiting. This is due to inhibition of hydrogen consumption by the presence of acetate.

The implications of this analysis is that there is a unique steady-state H_2 concentration, designated $\bar{H}_2$, that occurs for acetate concentrations below K_S^c, independent of the Fe(III) concentration and of whether there is any inhibition occurring between the acetate and hydrogen. While $\bar{H}_2$, which is predicted by eq 14 using the laboratory-derived coefficients from this study (30 °C, and ferric citrate as Fe(III) source), is higher than hydrogen concentrations observed in the field (usually closer to 15 °C and solid-phase Fe(III)), this does provides a possible explanation why there are consistent ranges of H_2 concentrations in the field for a given TEAP. For field conditions, there must be a balance between H_2 and other electron donors present, and the terminal electron acceptor if it is limiting, for steady-state hydrogen concentrations to be achieved. In the subsurface, this balance is a complicated function of the rate-limited availability of these compounds. For example, H_2 availability is related to the fermentation rate of organic substrates (*34*), and the organic substrate availability may be rate limited, such as dissolution from a NAPL. Furthermore, the iron source used in these experiments was soluble ferric citrate. In aquifer sediments, Fe^{3+} availability may be rate-limited due to microbially mediated dissolution from more insoluble iron(III) oxides (*33*, *35*). From a numerical modeling standpoint, these rates would be included in eqs 11−13 and would affect the steady-state hydrogen concentration calculated through eq 14.

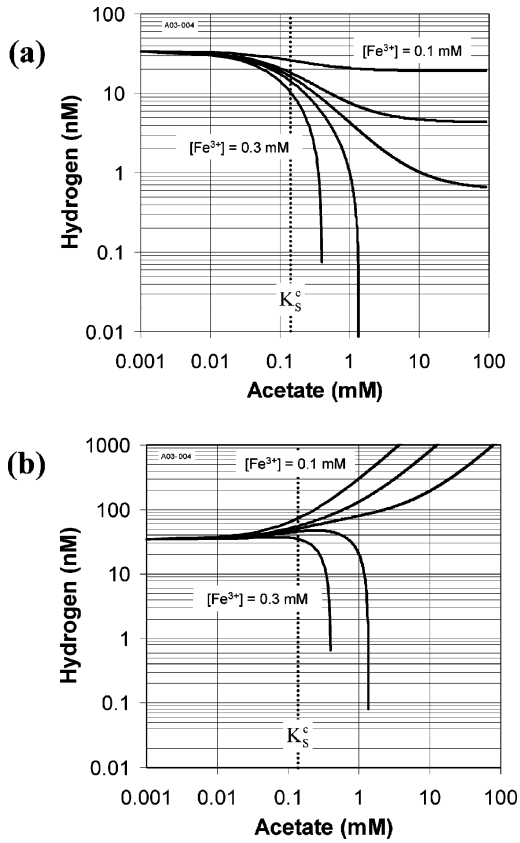

FIGURE 4. Steady-state aqueous hydrogen concentration as a function of acetate and Fe^{3+}. Fe^{3+} concentrations are 0.3, 0.25, 0.225, 0.2, and 0.1 mM. Curves calculated from eq 14 using coefficients in Table 1. Panel a is with no inhibition between electron donors, and panel b uses inhibition coefficients in Table 1. Dashed line is the Monod half-saturation constant for acetate degradation (Table 1).

The analyses presented here have shown that both the presence of a carbon source and limitations in the electron acceptor availability affect steady-state H_2 levels, but that for low carbon concentrations ($\ll K_S^c$) H_2 levels remain rather stable. Given the consistent H_2 levels found in groundwaters for a specific TEAP under a wide variety of conditions, this indicates that these H_2 levels in the field are rather robust and suggests that steady-state H_2 levels observed in aquifers cannot be predicted based on kinetic coefficients measured under ideal growth conditions in laboratory settings. The inability of the current data set to provide an accurate estimate of the K_s for H_2 uptake by *G. sulfurreducens* does not jeopardize this conclusion, since the available data suggest, as in the case of pure cultures of sulfate-reducing and methanogenic microorganisms, that the K_s for H_2 uptake by this organism under ideal growth conditions in the laboratory is likely to be in the micromolar rather than the nanomolar range.

Acknowledgments

The authors thank Dr. Derek Lovley for his contributions to this study, both in providing the *Geobacter sulfurreducens* culture used in the experimental work and in reviewing and providing valuable feedback on the manuscript. The authors also want to thank the anonymous reviewers for their excellent constructive comments on the manuscript. This research was funded by the Natural and Accelerated Bioremediation Research (NABIR) program, Biological and Environmental Research (BER), U.S. Department of Energy through Grant #DE-FG02-00ER63031, and by the National Science Foundation through CAREER Grant BES-0134362.

Supporting Information Available

Three figures. This material is available free of charge via the Internet at http://pubs.acs.org.

Literature Cited

(1) Chapell, F. H. *Ground-Water Microbiology and Geochemistry*, 2nd ed.; John Wiley & Sons: New York, 2001.

(2) Lovley, D. R.; Chapelle, F. H.; Woodward, J. C. Use of dissolved H_2 concentrations to determine distribution of microbially catalyzed reactions in anoxic groundwater. *Environ. Sci. Technol.* **1994**, *28*, 1205−1210.

(3) Lovley, D. R.; Goodwin, S. Hydrogen concentrations as an indicator of the predominant terminal electron accepting reactions in aquatic sediments. *Geochim. Cosmochim. Acta* **1988**, *52*, 2993−3003.

(4) Chapelle, F. H.; McMahon, P. B.; Dubrovsky, N. M.; Fujii, R. F.; Oaksford, E. T.; Vroblesky, D. A. Deducing the distribution of terminal electron-accepting processes in hydrologically diverse groundwater systems. *Water Resour. Res.* **1995**, *31*, 359−371.

(5) Champ, D. R.; Gulens, J.; Jackson, R. E. Oxidation−reduction sequences in ground water flow systems. *Can. J. Earth Sci.* **1979**, *16*, 12−23.

(6) Chapelle, F. H.; Haack, S. K.; Adriaens, P.; Henry, M. A.; Bradley, P. M. Comparison of Eh and H_2 measurements for delineating redox processes in a contaminated aquifer. *Environ. Sci. Technol.* **1996**, *30*, 3565−3569.

(7) Skubal, K. L.; Haack, S. K.; Forney, L. J.; Adriaens, P. Effects of dynamic redox zonation on the potential for natural attenuation of trichloroethylene at a fire-training-impacted aquifer. *Phys. Chem. Earth* **1999**, *24* (6), 517−527.

(8) Jakobsen, R.; Postma, D. Redox zoning, rates of sulfate reduction and interactions with Fe-reduction and methanogenesis in a shallow sandy aquifer, Romo, Denmark. *Geochim. Cosmochim. Acta* **1999**, *63* (1), 137−151.

(9) Schreiber, M. E.; Bahr, J. M. Spatial electron acceptor variability: implications for assessing bioremediation potential. *Biorem. J.* **1999**, *3* (4), 363−378.

(10) Robinson, J. A.; Tiedje, J. M. Competition between sulfate-reducing and methanogenic bacteria for H_2 under resting and growing conditions. *Arch. Microbiol.* **1984**, *137*, 26−32.

(11) Anderson, R. T.; Vrionis, H. A.; Ortiz-Bernad, I.; Resch, C. T.; Long, P. E.; Dayvault, R.; Karp, K.; Marutzky, S.; Metzler, D. R.; Peacock, A.; White, D. C.; Lowe, M.; Lovley, D. R. Stimulating the in situ activity of Geobacter species to remove Uranium from the groundwater of a Uranium-contaminated aquifer. *Appl. Environ. Microbiol.* **2003**, *69* (10), 5884−5891.

(12) Wilhelm, E.; Sattino, R.; Wilcock, R. J. Low-pressure solubility of gases in liquid water. *Chem. Rev.* **1977**, *77*, 219−262.

(13) Löffler, F. E.; Tiedje, J. M.; Sanford, R. A. Fraction of electrons consumed in electron acceptor reduction and hydrogen thresholds as indicators of halorespiratory physiology. *Appl. Environ. Microbiol.* **1999**, *65* (9), 4049−4056.

(14) Lovley, D. R. Bioremediation of organic and metal contaminants with dissimilatory metal reduction. *J. Ind. Microbiol.* **1995**, *14*, 85−93.

(15) Anderson, R. T.; Lovley, D. R. Microbial redox interactions with uranium: an environmental perspective. In *Interactions of Microorganisms with Radionuclides*; Keith-Roach, M. J., Livens, F. R., Eds.; Elsevier Science Ltd.: Amsterdam, 2002.

(16) Ahring, B. K.; Westermann, P.; Mah, R. A. Hydrogen inhibition of acetate metabolism and kinetics of hydrogen consumption by *Methanosarcina thermophila* TM-1. *Arch. Microbiol.* **1991**, *157*, 38−42.

(17) Boone, D. R.; Menaia, J. A. G. F.; Boone, J. E.; Mah, R. A. Effects of hydrogen pressure during growth and effects of pregrowth with hydrogen on acetate degradation by *Methanosarcina* species. *Appl. Environ. Microbiol.* **1987**, *53* (1), 83−87.

(18) Caccavo, F.; Lonergan, D. J.; Lovley, D. R.; Davis, M.; Stolz, J. F.; McInerny, M. J. *Geobacter sulfurreducens* sp. Nov., a hydrogen- and acetate-oxidizing dissimilatory metal-reducing microorganism. *Appl. Environ. Microbiol.* **1994**, *60*, 3752−3759.

(19) Lovley, D. R. Fe(III) and Mn(IV) reduction. In *Environmental Metal-Microbe Interactions*; Lovley, D. R., Ed.; ASM Press: Washington, DC, 2000.

(20) Snoeyenbos-West, O. L.; Nevin, K. P.; Anderson, R. T.; Lovley, D. R. Enrichment of *Geobacter* species in response to stimulation of Fe(III) reduction in sandy aquifer sediments. *Microb. Ecol.* **2000**, *39*, 153−167.

(21) Lovley, D. R.; Phillips, E. J. P. Novel mode of microbial energy metabolism: organic carbon oxidation coupled to dissimilatory reduction of iron or maganese. *Appl. Environ. Microbiol.* **1988**, *54*, 1472−1480.

(22) Lovley, D. R.; Phillips, E. J. P. Rapid assay for microbially reducible ferric iron in aquatic sediments. *Appl. Environ. Microbiol.* **1987**, *53*, 1536−1540.

(23) Liu, C.; Gorby, Y. A.; Zachara, J. M.; Fredrickson, J. K.; Brown, C. F. Reduction kinetics of Fe(III), Co(III), U(VI), Cr(VI), and Tc(VII) in cultures of dissimilatory metal-reducing bacteria. *Biotechnol. Bioeng.* **2002**, *80* (6), 637−649.

(24) Brown, D. G.; Guha, S.; Jaffé, P. R. Surfactant-enhanced biodegradation of a PAH in soil slurry reactors. *Biorem. J.* **1999**, *3* (3), 269−283.

(25) Guha, S.; Jaffe, P. R. Biodegradation kinetics of phenanthrene partitioned into the micellar phase of nonionic surfactants. *Environ. Sci. Technol.* **1996**, *30*, (2), 605−611.

(26) Liu, C.; Zachara, J. M.; Gorby, Y. A.; Szecsody, J. E.; Brown, C. F. Microbial reduction of Fe(III) and sorption/precipitation of Fe(II) on *Shewanella putrefaciens* strain CN32. *Environ. Sci. Technol.* **2001**, *35* (7), 1385−1393.

(27) Rittmann, B. E.; McCarty, P. L. *Environmental Biotechnology: Principles and Applications*; McGraw-Hill: New York, 2001.

(28) McCarty, P. L. Energetics of organic matter degradation. In *Water Pollution Microbiology*; Mitchell, R., Ed.; John Wiley & Sons: New York, 1972.

(29) Madigan, M. T.; Martinko, J. M.; Parker, J. *Brock: Biology of Microorganisms*, 8th ed.; Prentice-Hall: Upper Saddle River, NJ, 1997.

(30) Liu, C.; Zachara, J. M. Uncertainties of Monod kinetic parameters nonlinearly estimated from batch experiments. *Environ. Sci. Technol.* **2001**, *35* (1), 133−141.

(31) Vroblesky, D. A.; Chapelle, F. H. Temporal and spatial changes of terminal electron-accepting processes in a petroleum hydrocarbon-contaminated aquifer and the significance for contaminant biodegradation. *Water Resour. Res.* **1994**, *30*, 1561−1570.

(32) Vroblesky, D. A.; Bradley, P. M.; Chapelle, F. H. Influence of electron donor on the minimum sulfate concentration required for sulfate reduction in a petroleum hydroacrbon-contaminated aquifer. *Environ. Sci. Technol.* **1996**, *30*, 1377−1381.

(33) Chapelle, F. H.; McMahon, P. B.; Dubrovsky, N. M.; Fujii, R. F.; Oaksford, E. T. Rapid evolution of redox processes in a petroleum hydrocarbon-contaminated aquifer. *Ground Water* **2002**, *40*, 353−360.

(34) Logan, B. E.; Oh, S.-E.; Kim, I. S.; van Ginkel, S. Biological hydrogen production measured in batch anaerobic respirometers. *Environ. Sci. Technol.* **2002**, *36* (11), 2530−2535.

(35) Roden, E. E.; Wetzel, R. G. Kinetics of microbial Fe(III) oxide reduction in freshwater wetland sediments. *Limnol. Oceanogr.* **2002**, *47* (1), 198−211.

(36) Chapelle, F. H.; Vroblesky, D. A.; Woodward, J. C.; Lovley, D. R. Practical considerations for measuring hydrogen concentrations in groundwater. *Environ. Sci. Technol.* **1997**, *31* (10), 2873−2877.

Received for review September 6, 2004. Revised manuscript received January 18, 2005. Accepted January 27, 2005.

ES048613P